



## Al-Noor Journal of Engineering Management and Computer Science

ISSN: 3079-0689 (Online)

<https://njemcs.edu.iq/index.php/njemcs/>



# The Effects of Magnetic Nanofluid Flow with Different Heat Flux and Magnetic Field on Heat Transfer Through Horizontal Pipe

Ali Habeeb Askar<sup>1</sup>, Abdulhassan A. Karamallah<sup>1</sup>, Laith Jaafer Habeeb<sup>2</sup>

<sup>1</sup>University of Technology, Mechanical Engineering Department, Baghdad, Iraq.

<sup>2</sup>University of Technology, Training and Workshops Center, Baghdad, Iraq.

### ARTICLE INFO

#### Article history:

Received 03 November 2024,  
Revised 03 November 2024,  
Accepted 06 November 2024,  
Online 07 November 2024

#### Keywords:

Nanofluid  
Heat transfer  
Magnetic field  
Heat flux

### ABSTRACT

The influence of using nanoparticles with and without magnetic field on the characteristics of the flow and heat transfer rate is experimentally through a horizontal pipe. The base working fluid is distilled water, and the added nanoparticles are iron oxide ( $Fe_3O_4$ ), with a volume fraction of ( $\phi = 0.3, 0.6$  and  $0.9\%$ ). The intensity of the supplied magnetic field is (0.1 Tesla). The experiments are conducted at different heat fluxes (12.7, 15.9, 19.8  $kW/m^2$ ), two different inlet temperatures (23, 45  $^{\circ}C$ ), four different flow rates (2, 3, 3.5, 4, l/min) and range of Reynolds number (3930-7860). The results show that an increase in the concentration of nanofluids and heat flux give a boost in Nusselt number. Also, it is found that the use of a magnetic intensity enhances further heat transfer. The maximum enhancement in Nusselt number is about (18.3%) without using a magnetic field, and (20.1%) with the magnetic field, at a concentration of nanofluid of ( $\phi = 0.9\%$ ) and lower heat flux.


## 1. INTRODUCTION

Nanofluid is a suspension of nanoparticles such as  $Fe_3O_4$ -distilled water. The thermal conductivity of most solids is much higher than conventional heat transfer fluids. There have been proposed different techniques and methods to reduce the temperature of surfaces with a high heat transfer rate, and these techniques increase the heat transfer rate. The basis of these techniques covers the application of an electrical or a magnetic field, a vibration of a heated surfaced, structure variation or injection as well as the suction of a fluid, as proposed by Razi and Saedinia [1]. Al-dulaimy [2] performed a study of  $Al_2O_3$ /water nanofluid for studying

the laminar force convection with two different mass flow rates and heat flux of 150, 90, 50  $W/cm^2$ . An experimental study was evaluated by Saedinia and Nasr [3] with the principal aim to analyze the heat transfer rate as well as the pressure drop of a laminar flow nanofluid, specifically known as CuO/Base oil, this experiment was carried out with different insertions of coil in a tube and also, under a known and constant heat flux. Authors noticed that, on average, at highest Reynolds numbers inside the tube with wire coils inserted, the heat transfer coefficient is performed by 45%, whilst the pressure drop was diminished by 63%. Malvandi et al. [4] theoretically studied the migration of nanoparticles on a magneto-hydrodynamic

Corresponding author E-mail address: [Laith.J.Habeeb@uotechnology.edu.iq](mailto:Laith.J.Habeeb@uotechnology.edu.iq)

This work is an open-access article distributed under a CC BY license (Creative Commons Attribution 4.0 International) under

<https://creativecommons.org/licenses/by-nc-sa/4.0/> 

heat transfer by convection for a nanofluid denoted as alumina/water, flowing through the inlet side of a microchannel placed vertically. The boundary conditions were specified as a boundary subjected to varying heat fluxes, and the results demonstrated that nanoparticles were accumulated in the core zone of the heated walls, but also, they tend to accumulate to a region near to the lower heat transfer rate, which is near to the wall. Also, they stated that the asymmetric distribution of the nanoparticles increases the heat transfer rate because the nanoparticles performed velocities that produced a movement headed to the wall, which has higher thermal energy. On the other hand, Sheikholeslami *et al.* [5] conducted an experimental analysis of the heat transfer by means of forced convection in a lid-driven semi annulus enclosure filled with a nanofluid denoted as  $\text{Fe}_3\text{O}_4$ -water, with an asymmetric magnetic flux. The authors made the assumption that the fluid temperature increased linearly with the intensity of the magnetic flux as well as with the magnetization of the fluid. The governing equations were solved by vorticity-stream, a finite element method based on the management of the volume. The equations were solved for certain parameter such as the Hartmann, Reynolds and volume fraction of the nanoparticle varieties.

It was noticed from the authors that the Reynolds number variety increased linearly with the volume fraction of the nanoparticle, but the contrary happened with the Hartmann variety.

Also, was experimentally analyzed by Hatami *et al.* [6] that the magnetic flux under forced convection heat transfer for a nanofluid, denoted as  $\text{Fe}_3\text{O}_4$ -water, with a laminar flow behavior contained in a pipe placed horizontally and under constants heat fluxes. The authors measured the heat transfer rate by means of convection inside a pipe subjected to heat flux, as previously mentioned, with a magnetic fluid flowing through it and they noticed that the dimensions of the  $\text{Fe}_3\text{O}_4$  nanoparticles were approximately 100 nm with different concentrations and well distributed in the water. Their results showed

an external flux,  $Ha$ , between  $33.4 \times 10^{-4}$  and 136.6, and with a concentration of nanoparticles of 1%, 0.5%, 0.1% and 0%, which allowed to study the characteristics of the heat transfers. Also, the results of this investigation demonstrated that the presence of heat flux in the pipe increases the concentration of nanoparticles, which caused a diminishing in the heat transfer coefficient. Was also studied the heat transfer without an external flux, and was observed that the addition of magnetic nanoparticles enhanced the convection heat transfer 60 times. Moreover, it was appreciated that the Nusselt variety was diminished with an increase in the Hartmann variety for a specified magnetic nanofluid concentration, and this reduced the heat transfer rate 25 times. On the other hand, Karamallah *et al.* [7] conducted an experimental analysis on the distilled water flow and nanofluids, as well as in the heat transfer rate for concentrations of 0.9%, 0.6% and 0.3% in a pipe placed horizontally and subjected to a uniform magnetic field. The authors performed the experimental analysis with a varying Reynolds number from 2900 to 9820 and using a uniform heat flux from  $11262 \text{ W/m}^2$  to  $19562 \text{ W/m}^2$ . They noticed that the concentration of the nanofluid, the Nusselt number as well as the intensity of the magnetic field rose. The maximum percentage increases of the Nusselt Number with a magnetic nanofluid were 42.7%, 26.4% and 5.4% for volume concentrations of 0.9%, 0.6% and 0.3% respectively. Also, with a volume concentration of 0.9%, the enhancement of the intensity of the magnetic field was 0.1, 0.2 and 0.3 Tesla, with percentage increases of 43.

9%, 44.3% and 46% respectively. The enhancement on the heat transfer rate decreased as the Reynolds number increased when the magnets were used. On the other hand, the friction factor raised its magnitude when the volume concentration increased, whilst the magnet intensity diminished with an increase of the Reynolds number. A similar study was performed by Goharkhah *et al.* [8] in order to experimentally study the

conduction heat transfer rate of a ferrofluid subjected to dynamic conditions. The experiment consisted in the analysis of the heat transfer rate strength by means of conduction of the nanofluid known as Fe<sub>3</sub>O<sub>4</sub>/water ferrofluid moving through a pipe subjected to a uniform heat flux with several Reynolds number from 400 to 800 and a volume fraction from 1% to 2%. The results demonstrated that the heat transfer rate by means of conduction increased when the concentration of the nanofluids also increased. Moreover, was also appreciated by the authors that a heat flux of zero enhances the conduction heat transfer rate with an increase in the Reynolds variety, whilst the opposite behavior was observed when the system was subjected to a heat flux. In comparison to the thermal conduction in the water, the higher heat transfer rate by means of conduction increase of 32.3% for a

ferrofluid with 2 Vol% of concentration at a variety Reynolds Number of 400 and under a magnetic flux with a magnitude of 800 G was observed.

In this work, our contribution was to apply different heat flux on the pipe to observe the effect of heat transfer enhancement by using different magnetic field with magnetic oxide Fe<sub>3</sub>O<sub>4</sub>.

## 2. NANOFLUID PREPARATION AND PROPERTIES

The nanoparticles and the distilled water are mixed directly by a mixer with (2400 rpm) for 20 minutes before each experiment, the volume fraction used in the experiments are ( $\phi = 0, 0.3, 0.6$  and  $0.9$  % by volume). The test rig was performed by using a volume of water of 5 L. Equation (1) specifies the percentage relation for the determination of the volume concentration:

$$\phi = \frac{\text{volume of nanoparticle}}{\text{volume of nanoparticle} + \text{volume of water}} \times 100 \quad (1)$$

$$\phi = \frac{(m/\rho)_{\text{nanoparticle}}}{(m/\rho)_{\text{nanoparticle}} + (m/\rho)_{\text{water}}} \times 100 \quad (2)$$

The properties of nanoparticle and base fluid (viscosity, specific heat and density) are listed in Table (1).

TABLE 1: MATERIAL PROPERTIES [9].

Substance	Averagediameter (nm)	Density (Kg/m <sup>3</sup> )	Thermal conductivity (W/m.K)	Specific heat (J/kg.K)	Viscosity (pa.s)
Fe <sub>3</sub> O <sub>4</sub>	80	5180	80.4	670	-
Water	-	997	0.607	4180	0.000891

The measurement of the density, as well as the specific heat of a nanofluid, can be performed by applying the mixture laws of convection shown in equations (3) and (4) [9]:

$$C_{nf} = (1 - \phi)C_{bf} + \phi C_{np} \quad (3)$$

$$\rho_{nf} = (1 - \phi)\rho_{bf} + \phi\rho_{np} \quad (4)$$

Brickman [10] presented a viscosity correlation as it applies to concentrated particle suspension:

$$\mu_{nf} = \left( \frac{\mu_{bf}}{(1+\phi)^{2.5}} \right) \quad (5)$$

In order to determine the thermal conductivity, the Waspm model is taken into account [11]:

$$K_m = K_f \left[ \frac{2 + K_{pf} + 2\phi(K_{pf} - 1)}{2 + K_{pf} - \phi(K_{pf} - 1)} \right] \quad (6)$$

Where:

$$K_{pf} = \frac{K_p}{K_f} \quad (7)$$

## 3. EXPERIMENTAL SETUP

The experiment was carried out with a tube of copper of (0.014, 0.0158 m) inner and outer diameters and (1.5 m) test section length, helical heat exchanger nanofluid tank, pumps, flow meters, thermorecorder, variac, electric board, magnets and fittings, as shown in Figure 1.

The copper tube is heated uniformly by wrapping with Nichrome heater of 2000 watt. To generate a uniform heat flux, the outer layer of the pipe was subjected to an electrical current using a coil. An electric insulator of fiberglass is winding over the tube. Drilled ceramic bead elements are inserted around the wire heater to insulate the electrical heater, and then the wire heater is wined around the tube. An Aluminum foil and sectional pipe insulation glass wool type are used to decrease the heat despite. The temperature was measured by using eight thermocouples (k-type), which allowed determining the temperature in different test rig points. On the other hand, in

order to measure the temperature along the outer layer of the tube heated section, six thermocouples were used. The thermocouples are located along the test section with a space distance of (22 cm) between each one. To measure the fluid temperatures at the inlet and the outlet of the pipe, two immersed thermocouples were used. A stainless steel tank of (24 L) capacity is used to feed the pump with the required amount of working fluid. The spiral heat exchanger consisted of a copper tube coil with a diameter of 0.0125 m and a length of 15 m, applied to diminish the temperature of the hot stream coming from the test section. In a tank filled with re-circulating water, with a capacity of 125 L and made of stainless steel, was placed a coil. To measure the pressure drop along the test section, a manometer U-Tube type with CCL<sub>4</sub>, Carbon Tetrachloride, was used. Magnet is used in this experimental work, as illustrated in Table 2. It is measured by researchers using gauss meter.

**TABLE 2: STRENGTH OF THE MAGNET.**

Type of magnet	Number of magnets used	Strength of magnet at the surface (Gauss)	Strength at the center of pipe (20 mm) (Gauss)
Ferrite	5	1000	600

The experiments are done with distilled water, nanofluid: Iron Oxide (Fe<sub>3</sub>O<sub>4</sub>- distilled water) with volume fraction ( $\phi = 0.3, 0.6$  and  $0.9$  % by volume), magnetic field with each concentration with intensity (0.1 Tesla), Different constant heat flux (12.7, 15.9, 19.8 kW/m<sup>2</sup>), different inlet

temperature (23, 45) °C. All these tests are performed under a turbulent flow at the entrance, with magnitudes of Reynolds Number from 3930 to 7860), heat fluxes of 12.7 to 19.8 kW/m<sup>2</sup> and flow rates of 2, 3, 3.5 and 4 L/min.

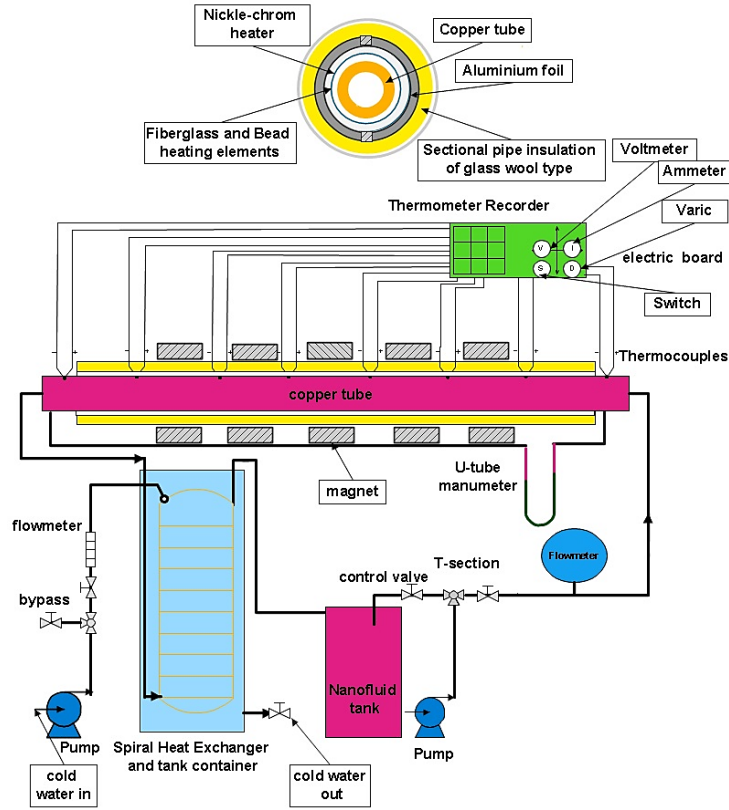


Figure 1: Diagram of experimental apparatus

#### 4. DATA REDUCTION

Equation (8) specifies the heat transfer rate produced by an electrical current, which is the heat flux applied to the outer layer of the tube:

$$P = V \times I \quad (8)$$

The heat transfer rate exchanged to the nanofluid from the heating wire can be determined by applying equation (9):

$$Q_{nf} = \dot{m} \times C_{nf} \times (T_o - T_i) \quad (9)$$

The balance between the heat input  $P$  and the nanofluid  $Q_{nf}$  can be computed by using equation (10), which common values are under 10%:

$$\dot{q} = \frac{Q_{nf}}{A_s} = \frac{2\pi k \Delta x [T_{so}(x) - T_{si}(x)]}{\pi D \Delta x \times \ln\left(\frac{r_o}{r_i}\right)} = \frac{2k [T_{so}(x) - T_{si}(x)]}{D \times \ln\left(\frac{r_o}{r_i}\right)} \quad (12)$$

The mean bulk fluid temperature,  $T_m(x)$  at the section ( $x$ ):

$$dq = q'' p dx = \dot{m} C_{nf} dT_m \quad (13)$$

$$\eta = \frac{P - Q_{nf}}{P} < 10 \% \quad (10)$$

The heat flux is given by:

$$\dot{q} = \frac{Q_{nf}}{A_s} = \frac{Q_{nf}}{\pi D_o L} \quad (11)$$

The following steps indicate the process to determine the local heat transfer coefficient:

1. The following values are known:  $\{\dot{q}, T_{so}(x)\}$ .
2. The temperature on the outer surface of the tube,  $T_{si}(x)$ , can be determined from the following equation [11]:

Where  $p = \pi D_i$  is the

$$dT_m = \frac{q'' \pi D_i}{\dot{m} C_{nf}} dx \quad (14)$$

The changes of the mean bulk fluid temperature in the function of the position  $x$  are computed by the integration of equation (14). The limits of the integration are from 0 to  $x$ , and this yields to:

$$T_m(x) = T_i + \frac{(T_o - T_i)}{L} x \quad (15)$$

Hence, the local heat transfer coefficient is computed from equation (16):

$$h(x) = \frac{\dot{q}}{T_{si}(x) - T_m(x)} \quad (16)$$

The local Nusselt Number is given by [2]:

$$Nu(x) = \frac{h_x D}{k_{nf}} \quad (17)$$

Equation (18) can be used to determine the mean Nusselt Number for the thermal developing zone:

$$Nu = \frac{1}{L} \int_0^L Nu(x) dx \quad (18)$$

From the empirical correlation of Gnielinski's [12], shown in equation (19), the experimental magnitudes of the Nusselt Number were compared:

$$Nu = \frac{(\frac{f}{2})(Re-1000)Pr}{1+12.7(\frac{f}{2})^{0.5}\left(\frac{Pr}{Pr^2-1}\right)} \quad (19)$$

and represented in figure (2)

Where

$$f = (1.58 \ln Re - 3.82)^{-2} \text{ for } 2300 < Re < 5 \times 10^6, 0.5 < Pr < 2000$$

## 5. Experimental Friction Factor

The Darcy Friction Factor can be determined by using equation (20), which is based on the pressure drop:

$$f = \frac{2 \times \Delta p \times D}{L \times \rho \times u^2} \quad (20)$$

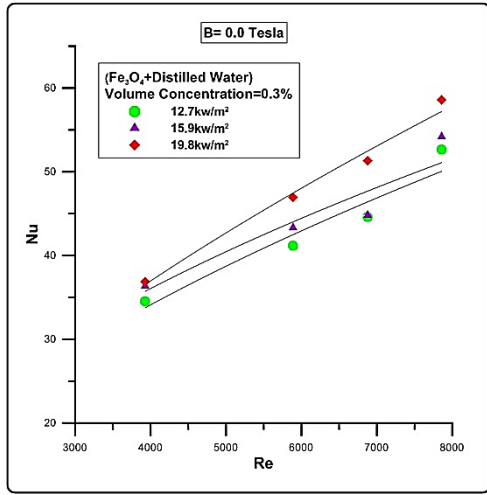
Where:

$$\Delta P = \gamma_{nf} \left( \frac{\rho_{CCl4}}{\rho_{nf}} - 1 \right) \times H \quad (21)$$

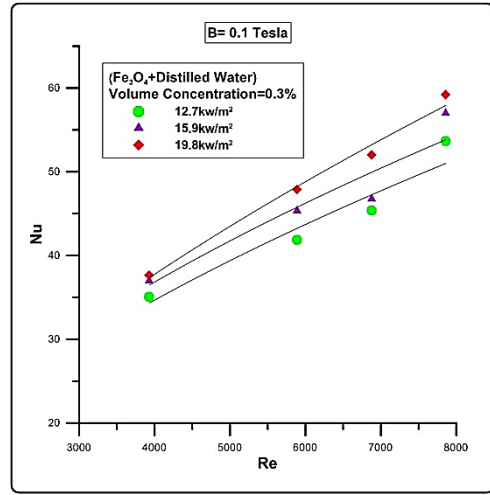
This is the pressure drop across the test section. The comparison of the present work with Gnielinski's and Blasius equation ( $f = 0.316 Re^{-0.25}$ ) for distilled water, to validate the rig performance, show good agreement.

## 6. RESULTS AND DISCUSSION

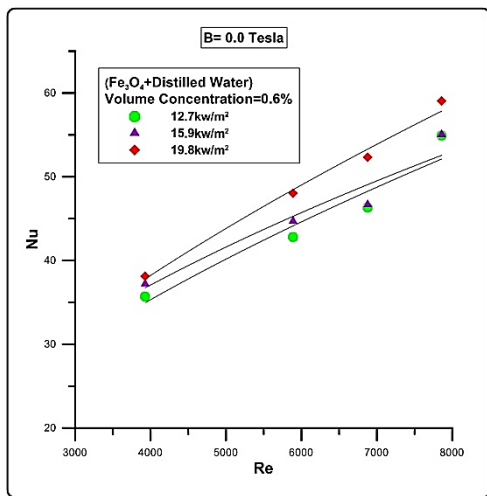
The Nusselt Number variation with the Reynolds Number at different uniform heat fluxes and (a, b, c), using a volume concentration of 0.3%, 0.6% and 0.9%, respectively, and shown in Figures 2 without magnetic and Figures 3 with magnetic field with strength (0.1 Tesla) the increase in heat flux, volume concentration, Reynold number, and magnetic field due to increase in Nusselt number and enhanced heat transfer. The average Nusselt number is increasing with increase ferrofluid volume concentration and with increase magnetic intensity for each concentration, and increases with increased Reynolds number, because, the effective thermal conductivity of nanofluid increases with the increasing volume fraction of the nanoparticles, shown in Figures 4 and 5. The effect of heat flux (nanoparticle migration from the surface with increase heat flux) with the magnetic field is due to viscous sublayer become very small (at entrance region) and accumulate the particle on surface increasing in fraction all these reasons due to enhanced in heat transfer. The effect of inlet temperature on heat transfer is noticed that when the temperature increases the heat transfer decrease shown in Figure 6 and the friction factor decrease when temperature increase is shown in Figure 7.



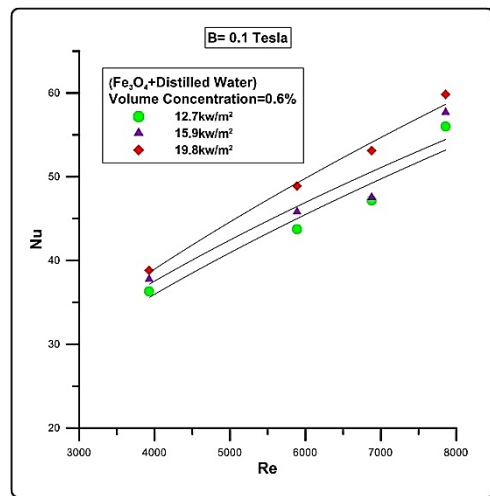
(a)



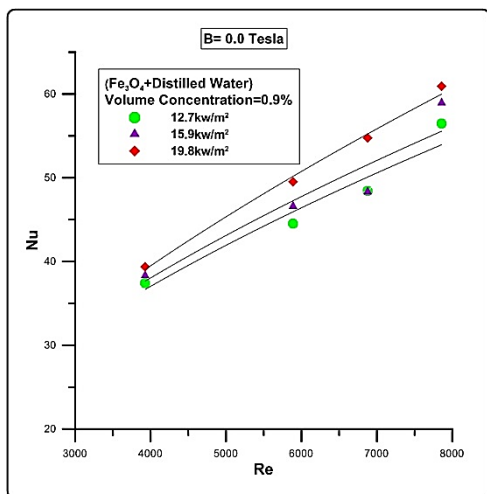
(a)



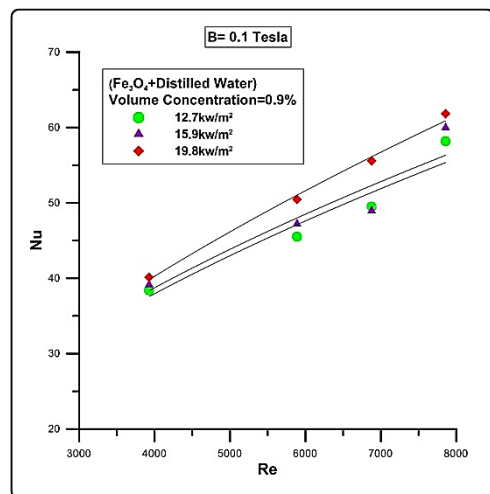
(b)



(b)



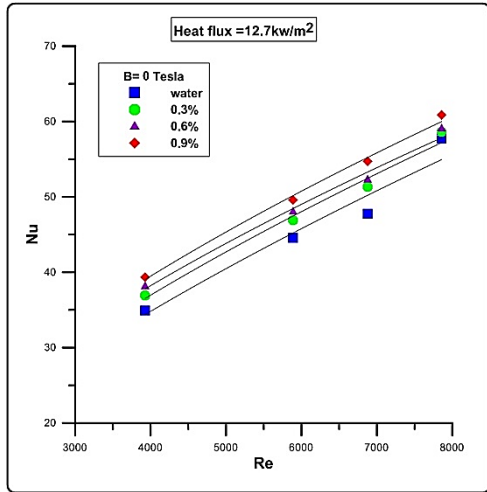
(c)



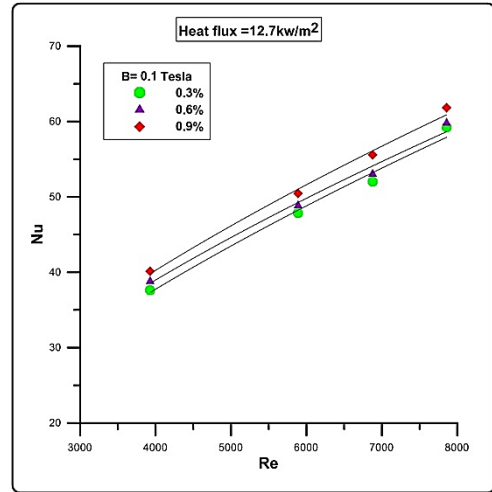
(c)

**Figure 2:** The effect of Reynolds number on average Nusselt number with different constant heat flux and without magnets.

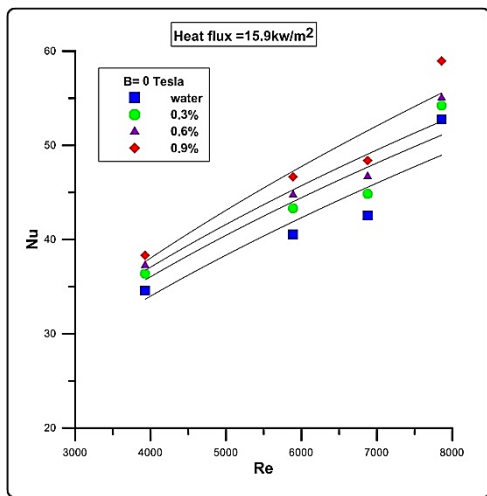
**Figures 3:** The effect of Reynolds number on average Nusselt number with different constant heat flux and with magnets.



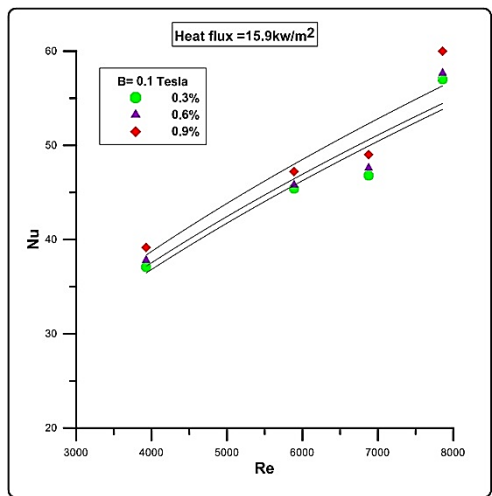
(a)



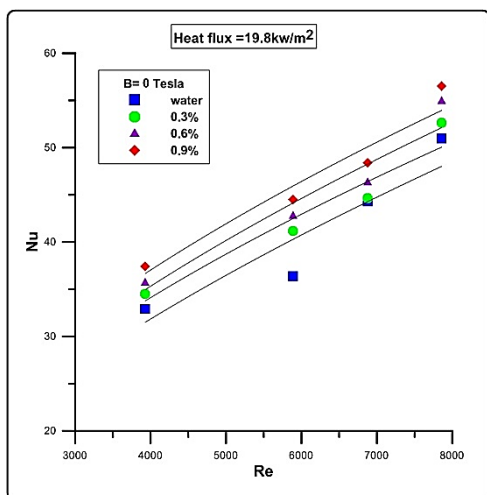
(a)



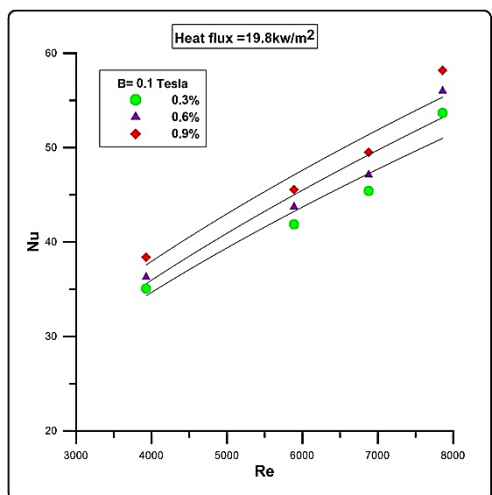
(b)



(b)



(c)



(c)

**Figures 4:** The effect of Reynolds number on Nusselt number with different constant heat flux, volume concentration and without magnets.

**Figures 5:** The effect of Reynolds number on Nusselt number with different constant heat flux, volume concentration and with magnets.

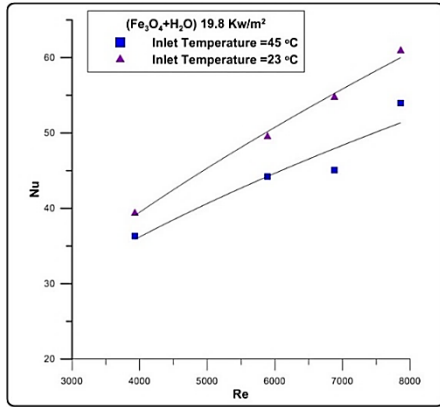


**Figure 6:** The effect of Reynolds on Nusselt number with different inlet temperature and Volume concentration =0.9% and constant heat flux =19.8Kw.m2.

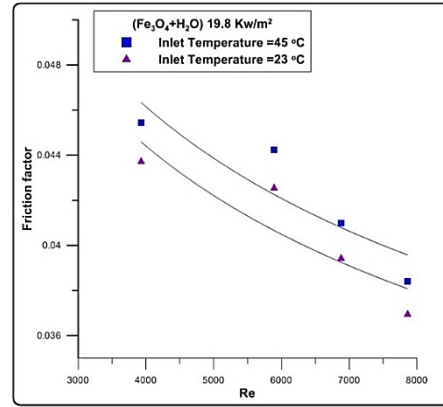
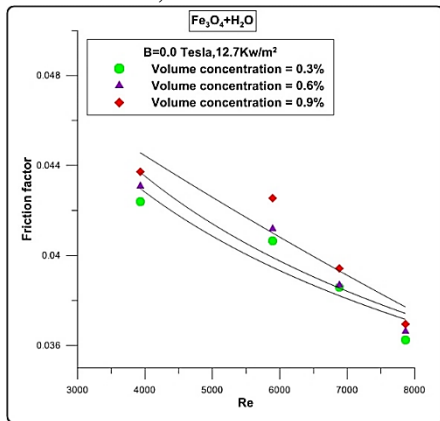


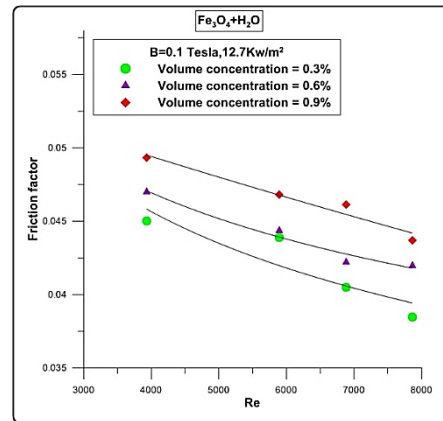
**Figure 7:** the effect of Reynolds on friction factor with different inlet temperature and Volume concentration =0.9% and constant heat flux =19.8Kw.m2.

The pressure drop is increasing with increase Reynolds number, ferrofluid concentration and the magnetic field intensity. It was appreciated that the friction factor raised its magnitude when the volume concentration and the intensity of the magnet increased, and the friction factor

diminished its magnitude when the Reynolds number decreased, as illustrated in Figure 8 and 9. The increase in the Nusselt Number of the magnetic nanofluid with respect to the water reaches the maximum value presented in Table 3.



**Figures 8:** The effect of Reynolds number on friction factor without magnets at different constant heat flux.



**Figures 9:** The effect of Reynolds number on friction factor with magnets at different constant heat flux.

**Table 3:** The maximum value of the enhancement.

Volume concentration %	Enhancement % with B=0.0 Tesla			Enhancement % with B=0.1 Tesla		
	Heat flux Kw/m <sup>2</sup>			Heat flux Kw/m <sup>2</sup>		
	12.7	15.9	19.8	12.7	15.9	19.8
0.3	11.6	6.4	6.9	13	10	8.2
0.6	14.98	9.5	8.6	16.7	11.5	9.9
0.9	18.3	13.1	12.7	20.1	14.1	13.9

## 7. CONCLUSIONS

The following points can be concluded from the present work:

1. The nanofluid employed, Fe<sub>3</sub>O<sub>4</sub> – distilled water with a particle size of 80 nm resulted in an enhancement in the heat transfer as well as in the Nusselt Number. The nanoparticles give higher heat transfer characteristics than the base fluid (distilled water). The maximum enhancement is (20.1%) established for magnetic nanofluid with concentration 0.9% and magnetic field 0.1 Tesla with heat flux 12.7 kW/m<sup>2</sup> and the minimum enhancement is (1.5%) established for magnetic nanofluid with concentration 0.3% without magnetic field with heat flux 19.8 kW/m<sup>2</sup>.
2. An increase in the concentration of the nanoparticles enhances the heat transfer rate.
3. The application of a magnetic field also increases the heat transfer enhancement, because the magnetic field gives higher Nusselt number compared to water-distilled and magnetic nanofluid.
4. The heat transfer decrease with increase inlet temperature.

**ACKNOWLEDGMENTS:** Authors would like to thank University of Technology/Mechanical Engineering Department and Training and Workshop Center for their support.

## NOMENCLATURE

$A_s$	Cross-sectional area (m <sup>2</sup> ).
$B$	Magnetic field (Tesla).
$C$	Specific heat (J/kg.K).
$D$	Diameter (m).
$f$	Friction factor.
$h$	Heat transfer coefficient (W/m <sup>2</sup> .K).
$I$	Electric Current (A).
$k$	Thermal conductivity (W/m.K).
$l$	Length of the test section (m).
$\dot{m}$	Mass flow rate (kg/s).
$Nu$	Nusselt number (-).
$Pr$	Prandtl number (-).
$Q$	Heat transfer rate (W).

$q$	Heat flux (W/m <sup>2</sup> ).
$r$	Radius of pipe (m).
$Re$	Reynolds number (-).
$T$	Temperature (K).
$t$	time (sec).
$u$	Velocity (m/s).
$V$	Voltage (volts).
$\gamma$	Specific weight.
$\Delta P$	Pressure drop across the tube.
$\rho$	Mass density (kg/m <sup>3</sup> ).
$\varphi$	Volume fraction of nanofluid.

## SUBSCRIPTS

$CCl_4$	Carbon tetrachloride
$f$	fluid
$H$	heat
$(i,o,s)$	in , out ,surface
$m$	mean
$n_f$	Nanofluid
$P$	Particle
$pf$	Particle fluid
$V$	vessel (aluminum vessel)
$W$	water
$X$	Distance

## REFERENCES

- [1] Razi, P., Akhavan-Behabadi, M.A. and Saeedinia, M., 2011. Pressure drop and thermal characteristics of CuO–base oil nanofluid laminar flow in flattened tubes under constant heat flux. *International Communications in Heat and Mass Transfer*, 38(7), pp.964-971.
- [2] Al-Dulaimy, F.M.A., 2013. Heat Transfer Enhancement in MCHS using Al<sub>2</sub>O<sub>3</sub>/Water Nanofluid. *Tikrit Journal of Engineering Sciences*, 20(2), pp.1-12.
- [3] Saeedinia, M., Akhavan-Behabadi, M.A. and Nasr, M., 2012. Experimental study on heat transfer and pressure drop of nanofluid flow in a horizontal coiled wire inserted tube under constant heat flux. *Experimental Thermal and Fluid Science*, 36, pp.158-168.
- [4] Malvandi, A., Kaffash, M.H. and Ganji, D.D., 2015. Nanoparticles migration effects on

magnetohydrodynamic (MHD) laminar mixed convection of alumina/water nanofluid inside microchannels. *Journal of the Taiwan Institute of Chemical Engineers*, 52, pp.40-56.

- [5] Sheikholeslami, M., Rashidi, M.M. and Ganji, D.D., 2015. Effect of non-uniform magnetic field on forced convection heat transfer of Fe<sub>3</sub>O<sub>4</sub>-water nanofluid. *Computer Methods in Applied Mechanics and Engineering*, 294, pp.299-312.
- [6] Hatami, N., Banari, A.K., Malekzadeh, A. and Pournafard, A.R., 2017. The effect of magnetic field on nanofluids heat transfer through a uniformly heated horizontal tube. *Physics Letters A*, 381(5), pp.510-515.
- [7] Karamallah, A.A., Habeeb, L.J. and Asker, A.H., 2016. The Effect of Magnetic Field with Nanofluid on Heat Transfer in a Horizontal Pipe. *Al-Khwarizmi Engineering Journal*, 12(3), pp.99-109.
- [8] Goharkhah, M., Gharekhani, S., Fallah, S. and Ashjaee, M., 2019. Dynamic measurement of ferrofluid thermal conductivity under an external magnetic field. *Heat and Mass Transfer*, 55(6), pp.1583-1592.
- [9] Sundar, L.S., Naik, M.T., Sharma, K.V., Singh, M.K. and Reddy, T.C.S., 2012. Experimental investigation of forced convection heat transfer and friction factor in a tube with Fe<sub>3</sub>O<sub>4</sub> magnetic nanofluid. *Experimental Thermal and Fluid Science*, 37, pp.65-71.
- [10] Brinkman, H.C., 1952. The viscosity of concentrated suspensions and solutions. *The Journal of Chemical Physics*, 20(4), pp.571-581.
- [11] Wasp F.J., *Solid-Liquid Slurry Pipeline Transportation*, Trans. Tech., 1977.
- [12] Gnielinski, V., 1976. New equations for heat and mass transfer in turbulent pipe and channel flow. *Int. Chem. Eng.*, 16(2), pp.359-368.
- [13] Holman, J.P., *Heat Transfer*, 10<sup>th</sup> ed. Mc-GrawHill Higher education, USA, 2010.
- [14] White, F. M., *Fluid Mechanics*, 4<sup>th</sup> ed., MacGraw-Hill books, USA, 2001.